

Nonlinear model reduction of dynamical power grid models using quadratization and balanced truncation

Tobias K. S. Ritschel, Frances Weiß, Manuel Baumann, and Sara Grundel

Abstract

In this work, we present a nonlinear model reduction approach for reducing two commonly used nonlinear dynamical models of power grids: the *effective network* (EN) model and the *synchronous motor* (SM) model. Such models are essential in real-time security assessments of power grids. However, as power grids are often large-scale, it is necessary to reduce the models in order to utilize them in real-time. We reformulate the nonlinear power grid models as quadratic systems and reduce them using balanced truncation based on approximations of the reachability and observability Gramians. Finally, we present examples involving numerical simulation of reduced EN and SM models of the IEEE 57 bus and IEEE 118 bus systems.

1 Introduction

Given a dynamical model, the purpose of model order reduction (MOR) is to identify another model which 1) can be analyzed more efficiently and 2) accurately captures the relevant dynamics and properties of the original model [3, 39]. Common analysis tasks include transient stability analysis, predictive simulation, uncertainty quantification, state estimation, and the solution of optimal control problems.

Power grids facilitate the delivery of electricity from producers to consumers. Modern power grids consist of 1) power plants, 2) transmission grids, 3) distribution grids, and 4) consumers (either industrial or residential). In recent years, emerging technologies such as renewable energy production, charging of electric vehicles, and *prosumers* have decreased the predictability of the power generation and consumption in power grids. Therefore, there is an increasing need to perform real-time grid security assessments. However, power grid networks are often large-scale, and the commonly used dynamical power grid models are

nonlinear [28]. Consequently, they are nontrivial to analyze in real-time. Therefore, model reduction (also called *equivalencing* [16, 26]) has long been used to reduce both static and dynamical models of power systems [9, 36, 50].

Balanced truncation is a model reduction technique that involves projecting the state variables and the dynamical equations such that the states that are least affected by the inputs are also the states that affect the outputs the least. These states do not significantly affect the input-output behavior of the system and can, thus, be removed.

In fact, most model reduction techniques involve projection and truncation [3], and for linear systems, the reduced system matrices can be computed offline. However, for general nonlinear systems, the evaluation of the reduced right-hand side function will also involve the evaluation of the original right-hand side function. If this is not addressed, the reduced nonlinear model can not be analyzed significantly more efficient than the original model.

Therefore, most research on model reduction of power grid models involves reduction of a linearized system or subsystem. Researchers have used, e.g., balanced truncation [1, 2, 8, 22, 35, 37, 40–44, 54], *balanced residualization* [32], *Krylov methods* [6, 38, 46, 47], *SVD-Krylov methods* [17], *proper orthogonal decomposition* (POD) [48], *singular perturbation theory* [10, 25, 31], variants of *clustering* [7, 14, 49], and sparse approximations [23] to reduce such linearized models.

However, nonlinear model reduction of power grid models has also been considered. Parrilo et al. [33] use POD and Lan et al. [21] and Zhao et al. [52, 53] use balanced truncation based on *empirical Gramians* to reduce nonlinear models of power grids. However, they do not describe how to efficiently evaluate the reduced right-hand side function. Malik et al. [24] use POD together with *trajectory piecewise linearization* (TPWL) to reduce a nonlinear power grid model, and Purvine et al. [34] use a clustering approach where each cluster is represented by a single generator. Osipov and Sun [29] and Osipov et al. [30] use a hybrid approach where only a subset of the original right-hand side functions are linearized. Finally, Mlinarić et al. [27] use concepts of synchronicity to derive exact nonlinear reduced power grid models.

Tobias K. S. Ritschel, Frances Weiß, Manuel Baumann, and Sara Grundel are with Max Planck Institute for Dynamics of Complex Technical Systems, D-39106 Magdeburg, Germany. E-mails: {ritschel, grundel}@mpi-magdeburg.mpg.de.

In this work, we use *lifting* [19, 20] to reformulate the *effective network* (EN) model and the *synchronous motor* (SM) model [28] as quadratic models. We use a balanced truncation approach, based on approximations of the reachability and observability Gramians of the quadratic systems [5, 51], to reduce the quadratized models. Since the systems are quadratic, we can compute the reduced system matrices offline. Consequently, the reduced models can be analyzed more efficiently than the original models. Finally, we present numerical examples which demonstrate the accuracy of the reduced models with numerical simulations of the IEEE 57 bus and the IEEE 118 bus systems. We use `pg_sync_models` [28] to obtain dynamical models of these systems.

The remainder of this paper is organized as follows. In Section 2, we describe the quadratization of the EN and SM models. In Section 3, we describe the balanced truncation approach for reducing the quadratized EN and SM models, and in Section 4, we present the numerical examples. Finally, conclusions are given in Section 5.

2 Power system models

The three commonly used dynamical models of power grid networks are the EN model, the SM model, and the *structure-preserving* (SP) model [28]. All three models represent the generators and the loads (i.e., the consumers) in the power grid network as a set of coupled oscillators. The phase angle of the i 'th oscillator (i.e., the i 'th state variable) is described by

$$\frac{2J_i}{\omega_R} \ddot{\delta}_i + \frac{D_i}{\omega_R} \dot{\delta}_i = F_i + f_i(\delta), \quad (1)$$

for $i = 1, \dots, n_o$ where n_o is the number of oscillators. Here, ω_R is a reference frequency, H_i is the inertia constant, and D_i is the damping constant of the i 'th oscillator. F_i is constant, and

$$f_i(\delta) = - \sum_{\substack{j=1 \\ j \neq i}}^{n_o} K_{ij} \sin(\delta_i - \delta_j - \gamma_{ij}) \quad (2)$$

is a nonlinear coupling term. The constant parameters F_i , K_{ij} , and γ_{ij} depend on the steady state power flow in the network, i.e., on the solution to the *power flow equations* [28].

Remark 1 *For the EN and SM models, $J_i \neq 0$ for all i . However, for the SP model, $J_i = 0$ for indices i representing load nodes. Consequently, the transformations described in this section would result in either 1) a quadratic differential-algebraic system or 2) a cubic system. Therefore, we consider only the EN and the SM models.*

2.1 Transformation to first-order system

In order to compute the Gramians in Section 3, it is necessary to transform the second-order system (1) to a first-order system by augmenting the state variables with the frequencies, $\omega := \dot{\delta}$:

$$\dot{\delta}_i = \omega_i, \quad (3a)$$

$$\dot{\omega}_i = -\frac{D_i}{2J_i} \omega_i + \frac{\omega_R}{2J_i} F_i + \frac{\omega_R}{2J_i} f_i(\delta), \quad (3b)$$

for $i = 1, \dots, n_o$.

2.2 Quadratization

We further augment the state variables by introducing $s := \sin(\delta)$ and $c := \cos(\delta)$ and use trigonometric identities to rewrite the nonlinear function (2):

$$f_i(s, c) = - \sum_{\substack{j=1 \\ j \neq i}}^{n_o} K_{ij} \left((s_i c_j - c_i s_j) \gamma_{ij}^c - (c_i c_j + s_i s_j) \gamma_{ij}^s \right). \quad (4)$$

$\gamma_{ij}^s := \sin(\gamma_{ij})$ and $\gamma_{ij}^c := \cos(\gamma_{ij})$. The nonlinear function (4) is quadratic in s and c . Furthermore, we use the chain rule to derive dynamical equations for s and c (which are also quadratic). The resulting lifted quadratic system is

$$\dot{\delta}_i = \omega_i, \quad (5a)$$

$$\dot{\omega}_i = -\frac{D_i}{2J_i} \omega_i + \frac{\omega_R}{2J_i} F_i + \frac{\omega_R}{2J_i} f_i(s, c), \quad (5b)$$

$$\dot{s}_i = c_i \omega_i, \quad (5c)$$

$$\dot{c}_i = -s_i \omega_i, \quad (5d)$$

for $i = 1, \dots, n_o$.

Remark 2 *The right-hand sides of the lifted quadratic system (5) are independent of the phase angles, δ .*

2.2.1 Matrix form

The quadratic system (5) is in the form

$$\dot{x} = Ax + H(x \otimes x) + Bu, \quad (6)$$

where $x := [\delta; \omega; s; c] \in \mathbb{R}^{4n_o}$ are the state variables, $u \in \mathbb{R}$ is the scalar manipulated input, and \otimes denotes the Kronecker product [11, 15, 45]. We use the last term in (6) to represent the constant terms in (5). Consequently, the (constant) manipulated inputs, $u = 1$, do not represent physical manipulable quantities.

The system matrices in (6) have block structure:

$$A = \begin{bmatrix} A_{11} & \cdots & A_{14} \\ \vdots & \ddots & \vdots \\ A_{41} & \cdots & A_{44} \end{bmatrix} \in \mathbb{R}^{4n_o \times 4n_o}, \quad (7a)$$

$$H = \begin{bmatrix} H_{11} & \cdots & H_{14} \\ \vdots & \ddots & \vdots \\ H_{41} & \cdots & H_{44} \end{bmatrix} \in \mathbb{R}^{4n_o \times (4n_o)^2}, \quad (7b)$$

$$B = \begin{bmatrix} B_1 \\ \vdots \\ B_4 \end{bmatrix} \in \mathbb{R}^{4n_o \times 1}. \quad (7c)$$

$A_{ij} \in \mathbb{R}^{n_o \times n_o}$, $H_{ij} \in \mathbb{R}^{n_o \times 4n_o^2}$, and $B_i \in \mathbb{R}^{n_o \times 1}$.

The nonzero blocks in A are

$$A_{12} = I, \quad (8a)$$

$$A_{22} = -\frac{1}{2}J^{-1}D, \quad (8b)$$

where I is the identity matrix, $J = \text{diag}\{J_i\}_{i=1}^{n_o}$, and $D = \text{diag}\{D_i\}_{i=1}^{n_o}$.

The nonzero blocks of the Hessian matrix, H , are block-diagonal where each block is a row vector with $4n_o$ elements:

$$H_{23} = \text{blkdiag} \left\{ \left[0 \quad 0 \quad \frac{\omega_{\beta}}{2J_i} h_i^s \quad -\frac{\omega_{\beta}}{2J_i} h_i^c \right]_{i=1}^{n_o} \right\}, \quad (9a)$$

$$H_{24} = \text{blkdiag} \left\{ \left[0 \quad 0 \quad \frac{\omega_{\beta}}{2J_i} h_i^c \quad \frac{\omega_{\beta}}{2J_i} h_i^s \right]_{i=1}^{n_o} \right\}, \quad (9b)$$

$$H_{34} = \text{blkdiag} \left\{ \left[0 \quad e_i \quad 0 \quad 0 \right]_{i=1}^{n_o} \right\}, \quad (9c)$$

$$H_{43} = \text{blkdiag} \left\{ \left[0 \quad -e_i \quad 0 \quad 0 \right]_{i=1}^{n_o} \right\}. \quad (9d)$$

The i 'th element of the row vector $e_i \in \mathbb{R}^{n_o}$ is one, and all other elements are zero. The elements of the row vectors $h_i^s, h_i^c \in \mathbb{R}^{n_o}$ are

$$h_{ij}^s = \begin{cases} K_{ij} \gamma_{ij}^s, & j \neq i, \\ 0, & j = i, \end{cases} \quad (10a)$$

$$h_{ij}^c = \begin{cases} K_{ij} \gamma_{ij}^c, & j \neq i, \\ 0, & j = i. \end{cases} \quad (10b)$$

Finally, the nonzero block of B is

$$B_2 = F. \quad (11)$$

Remark 3 *The Hessian matrix, H , is not unique. Therefore, we modify it such that it is symmetric [4], i.e., such that $H(u \otimes v) = H(v \otimes u)$.*

2.3 Nonzero initial condition

In Section 3, we use expressions for the Gramians of quadratic systems which require that the initial condition is zero [5]. However, the state variables in the lifted quadratic model contain both sines and cosines of the phase angles. These can not simultaneously be zero. Therefore, we introduce the shifted state variables $\bar{x} := x - x_0$ and the augmented manipulated inputs $\bar{u} := [u; 1]$. x_0 is a given initial condition for the lifted quadratic system. Using properties of the Kronecker product [15], we derive a quadratic model for the shifted state variables (which are zero at the initial time):

$$\dot{\bar{x}} = \bar{A}\bar{x} + H(\bar{x} \otimes \bar{x}) + \bar{B}\bar{u}, \quad \bar{x}(0) = 0. \quad (12)$$

In (12), $\bar{A} = A + A_0$ and $\bar{B} = [B \quad B_0]$, where

$$A_0 = H((I \otimes x_0) + (x_0 \otimes I)), \quad (13a)$$

$$B_0 = Ax_0 + H(x_0 \otimes x_0). \quad (13b)$$

3 Model reduction

In this section, we describe a balanced truncation approach, based on that described by Benner and Goyal [5], for reducing the quadratic system

$$\dot{x} = Ax + H(x \otimes x) + Bu, \quad x(0) = 0, \quad (14a)$$

$$y = Cx, \quad (14b)$$

where $x \in \mathbb{R}^n$, $u \in \mathbb{R}^m$, $y \in \mathbb{R}^p$, $A \in \mathbb{R}^{n \times n}$, $H \in \mathbb{R}^{n \times n^2}$, $B \in \mathbb{R}^{n \times m}$, and $C \in \mathbb{R}^{p \times n}$. (14a) is the shifted dynamical power system model described in Section 2, and (14b) relates the outputs, y , to the state variables, x .

In order to reduce (14), we use the projection matrices $\mathcal{W}, \mathcal{V} \in \mathbb{R}^{n \times n_r}$ ($\mathcal{W}^T \mathcal{V} = I$) to project and truncate the state variables ($x \approx \mathcal{V}\hat{x}$) and the dynamical equations (left multiply by \mathcal{W}^T). n_r is the number of states in the reduced model. The resulting quadratic reduced order model is

$$\dot{\hat{x}} = A_r \hat{x} + H_r(\hat{x} \otimes \hat{x}) + B_r u, \quad (15a)$$

$$\hat{y} = C_r \hat{x}, \quad (15b)$$

where $\hat{x} \in \mathbb{R}^{n_r}$ and $\hat{y} \in \mathbb{R}^p$ are the reduced state variables and outputs, and $A_r \in \mathbb{R}^{n_r \times n_r}$, $H_r \in \mathbb{R}^{n_r \times n_r^2}$, $B_r \in \mathbb{R}^{n_r \times m}$, and $C_r \in \mathbb{R}^{p \times n_r}$ are the reduced system matrices given by the projections

$$A_r = \mathcal{W}^T A \mathcal{V}, \quad (16a)$$

$$H_r = \mathcal{W}^T H(\mathcal{V} \otimes \mathcal{V}), \quad (16b)$$

$$B_r = \mathcal{W}^T B, \quad (16c)$$

$$C_r = C \mathcal{V}. \quad (16d)$$

Remark 4 *The Kronecker product $\mathcal{V} \otimes \mathcal{V} \in \mathbb{R}^{n^2 \times n_r^2}$ is prohibitively large in terms of memory requirements, even for moderately sized power grids.*

3.1 Gramians of quadratic systems

The reachability Gramian, P , and the observability Gramian, Q , of the quadratic system (14) (with zero initial condition) are [5]

$$P = \sum_{i=1}^{\infty} P_i, \quad (17a)$$

$$Q = \sum_{i=1}^{\infty} Q_i, \quad (17b)$$

where P_1 and Q_1 satisfy the Lyapunov equations

$$AP_1 + P_1A^T + BB^T = 0, \quad (18a)$$

$$A^TQ_1 + Q_1A + C^TC = 0, \quad (18b)$$

and P_i and Q_i satisfy the Lyapunov equations

$$AP_i + P_iA^T + H \left(\sum_{k=1}^{i-2} P_k \otimes P_{i-(k+1)} \right) H^T = 0, \quad (19a)$$

$$A^TQ_i + Q_iA + \mathcal{H}^{(2)} \left(\sum_{k=1}^{i-2} P_k \otimes Q_{i-(k+1)} \right) (\mathcal{H}^{(2)})^T = 0, \quad (19b)$$

for $i \geq 2$. $\mathcal{H}^{(2)}$ denotes the mode-2 *matricization* of the tensor, $\mathcal{H} \in \mathbb{R}^{n \times n \times n}$, for which the mode-1 matricization, $\mathcal{H}^{(1)}$, is the Hessian matrix, H . Essentially, $\mathcal{H}^{(2)}$ is obtained by reordering the elements of H (see Appendix A).

Remark 5 For even values of i , the solution to (19) is $P_i = Q_i = 0$.

Remark 6 Benner and Goyal [5] showed that the reachability and observability Gramians (17) satisfy generalized Lyapunov equations and described an iterative scheme for solving these equations. However, the examples of power grid models considered in this work do not satisfy the convergence criteria for this scheme [5, Theorem 5.3 on page 23]. Therefore, we approximate the Gramians.

3.2 Approximation of the Gramians

We approximate the Gramians by truncating the sums in (17) to the first N terms. Furthermore, we use low-rank approximations to reduce the memory consumption, which is a key computational bottleneck because of the Kronecker products in (19). Finally, for the power system models described in Section 2, some eigenvalues of A are zero (whether the system is shifted to have zero initial condition or not). However, the real parts of the eigenvalues of

A must be strictly negative in order to guarantee the existence and uniqueness of solutions to the Lyapunov equations (18)-(19). Therefore, when computing the approximate Gramians, we replace A by a shifted matrix,

$$A_\alpha = A - \alpha I, \quad (20)$$

where $\alpha \in \mathbb{R}$ is small and positive.

We approximate the Gramians, P and Q , in (17), by 1) truncating the sums and 2) approximating the truncated sums, i.e., we approximate P by $P_T \approx \sum_{i=1}^N P_i \approx P$ and Q by $Q_T \approx \sum_{i=1}^N Q_i \approx Q$. The approximations are

$$P_T = \tilde{X}_N \tilde{X}_N^T, \quad (21a)$$

$$Q_T = \tilde{Z}_N \tilde{Z}_N^T, \quad (21b)$$

where \tilde{X}_N and \tilde{Z}_N are computed iteratively. $\tilde{X}_1 = \tilde{R}_1$ and $\tilde{Z}_1 = \tilde{S}_1$ where \tilde{R}_1 and \tilde{S}_1 are approximate low-rank factors of the solutions to (18). Next,

$$\tilde{X}_i = \mathcal{T}_\tau \left(\begin{bmatrix} \tilde{X}_{i-2} & \tilde{R}_i \end{bmatrix} \right), \quad (22a)$$

$$\tilde{Z}_i = \mathcal{T}_\tau \left(\begin{bmatrix} \tilde{Z}_{i-2} & \tilde{S}_i \end{bmatrix} \right), \quad (22b)$$

for $i = 3, 5, \dots, N$, where \tilde{R}_i and \tilde{S}_i are approximate low-rank factors of the solutions to (19), and $\mathcal{T}_\tau(\cdot)$ denotes low-rank approximation (see Appendix B).

We obtain the approximate low-rank factors by

$$\tilde{R}_i = \mathcal{T}_\tau(R_i), \quad (23a)$$

$$\tilde{S}_i = \mathcal{T}_\tau(S_i), \quad (23b)$$

where R_i and S_i are approximations of the Cholesky factors of the solutions to (18)-(19) satisfying

$$A_\alpha R_i R_i^T + R_i R_i^T A_\alpha^T + BB^T = 0, \quad (24a)$$

$$A_\alpha^T S_i S_i^T + S_i S_i^T A_\alpha + C^TC = 0, \quad (24b)$$

and

$$A_\alpha R_i R_i^T + R_i R_i^T A_\alpha^T + \tilde{K}_{i,i-2} \tilde{K}_{i,i-2}^T = 0, \quad (25a)$$

$$A_\alpha^T S_i S_i^T + S_i S_i^T A_\alpha + \tilde{L}_{i,i-2} \tilde{L}_{i,i-2}^T = 0, \quad (25b)$$

for $i = 3, 5, \dots, N$.

The third terms in (25) are approximations of the third terms in (19), and we compute $\tilde{K}_{i,i-2}$ and $\tilde{L}_{i,i-2}$ iteratively. $\tilde{K}_{i1} = \mathcal{T}_\tau(\Delta K_{i1})$ and $\tilde{L}_{i1} = \mathcal{T}_\tau(\Delta L_{i1})$, and

$$\tilde{K}_{ik} = \mathcal{T}_\tau \left(\begin{bmatrix} \tilde{K}_{i,k-2} & \Delta K_{ik} \end{bmatrix} \right), \quad (26a)$$

$$\tilde{L}_{ik} = \mathcal{T}_\tau \left(\begin{bmatrix} \tilde{L}_{i,k-2} & \Delta L_{ik} \end{bmatrix} \right), \quad (26b)$$

for $k = 3, 5, \dots, i-2$, where

$$\Delta K_{ik} = H \left(\tilde{R}_k \otimes \tilde{R}_{i-(k+1)} \right), \quad (27a)$$

$$\Delta L_{ik} = \mathcal{H}^{(2)} \left(\tilde{R}_k \otimes \tilde{S}_{i-(k+1)} \right). \quad (27b)$$

$\Delta K_{ik} \Delta K_{ik}^T$ approximates $H(P_k \otimes P_{i-(k+1)})H^T$, and $\Delta L_{ik} \Delta L_{ik}^T$ approximates $\mathcal{H}^{(2)}(P_k \otimes Q_{i-(k+1)})(\mathcal{H}^{(2)})^T$.

Finally, we use matricization to evaluate (27) efficiently (see Appendix C).

3.3 Balanced truncation

Based on numerical experiments, we project and truncate $\bar{\delta}$, $\bar{\omega}$, \bar{s} , and \bar{c} (the variables shifted to have zero initial condition), and their corresponding dynamical equations, separately. This corresponds to choosing block-diagonal projection matrices \mathcal{V} and \mathcal{W} . Furthermore, we use the same projection matrices, \mathcal{V}_ω and \mathcal{W}_ω , for all four variables:

$$\mathcal{V} = \text{blkdiag}\{\mathcal{V}_\omega, \mathcal{V}_\omega, \mathcal{V}_\omega, \mathcal{V}_\omega\}, \quad (28a)$$

$$\mathcal{W} = \text{blkdiag}\{\mathcal{W}_\omega, \mathcal{W}_\omega, \mathcal{W}_\omega, \mathcal{W}_\omega\}. \quad (28b)$$

We compute the projection matrices using the square-root algorithm [3] based on the second $n_o \times n_o$ diagonal blocks, $P_{\omega,T}$ and $Q_{\omega,T}$, of P_T and Q_T given by (21):

$$\mathcal{V}_\omega = R_\omega^T U_r \Sigma_r^{-1/2}, \quad (29a)$$

$$\mathcal{W}_\omega = S_\omega^T V_r \Sigma_r^{-1/2}. \quad (29b)$$

R_ω and S_ω are the Cholesky factors of $P_{\omega,T}$ and $Q_{\omega,T}$, and U_r and V_r consist of the first $n_r/4$ columns of U and V , respectively, where $R_\omega S_\omega^T = U \Sigma V^T$ is the singular value decomposition. Σ_r is a diagonal matrix with the $n_r/4$ largest singular values on the diagonal.

Remark 7 *Due to numerical errors, $P_{\omega,T}$ and $Q_{\omega,T}$ may not be positive definite. In that case, we 1) use the polar decomposition [12] to compute the nearest symmetric positive semidefinite matrix [13] and 2) add a small multiple of the identity matrix to ensure strict positive definiteness.*

3.4 Steady state adjustment

As mentioned in Remark 2, the right-hand sides of the original nonlinear first-order EN and SM models (3) are independent of the phase angles, δ . Consequently, ω , s , and c may reach steady state regardless of the dynamics of δ . Since $\dot{\delta} = \omega$, δ only reaches steady state if the frequencies, ω , are zero in steady state. This is the case for the original model. Otherwise, (5c) and (5d) could not simultaneously be in steady state, as s_i and c_i cannot both be zero.

These aspects lead to issues in the reduced model. We explain them and their solution assuming that the initial frequencies are $\omega_0 = 0$. In that case, the reduced phase angles are given by

$$\dot{\hat{\delta}} = \hat{\omega}. \quad (30)$$

Analogous to the original model, the right-hand sides of the reduced model are independent of $\hat{\delta}$. However, the reduced frequencies, $\hat{\omega}$, are not necessarily zero in steady state. Consequently, $\hat{\delta}$ will not reach steady state. Therefore, we shift the right-hand side of (30) by the steady

state of the reduced frequencies, $\hat{\omega}_s$:

$$\dot{\hat{\delta}} = \hat{\omega} - \hat{\omega}_s. \quad (31)$$

Consequently, when $\hat{\omega}$ reaches steady state, the right-hand side of (31) is zero, and $\hat{\delta}$ is also in steady state. The issues and the solution are similar if $\omega_0 \neq 0$ is used in the reduction, and we stress that we only shift the system once offline.

4 Numerical examples

In this section, we use numerical simulation to test the accuracy of reduced EN and SM models of the IEEE 57 bus system for different choices of parameters in the balanced truncation approach, initial conditions, and manipulated inputs. Furthermore, we demonstrate that we can effectively reduce the IEEE 118 bus system. Table 1 shows the number of coupled oscillators in the EN and SM models, i.e., the number of states in the original second-order model (1). We use the Matlab toolboxes MATPOWER 6.0 [55, 56] and pg_sync_models [28] to compute the parameters in the original model equations (1)-(2).

For all tests, we use the initial conditions $\delta_0 = \omega_0 = 0$ (such that $s_0 = 0$ and $c_0 = 1$) and the manipulated inputs $u = [1; 1]$ when we reduce the models. Furthermore, the (scalar) output, y , is the average of the phase angles.

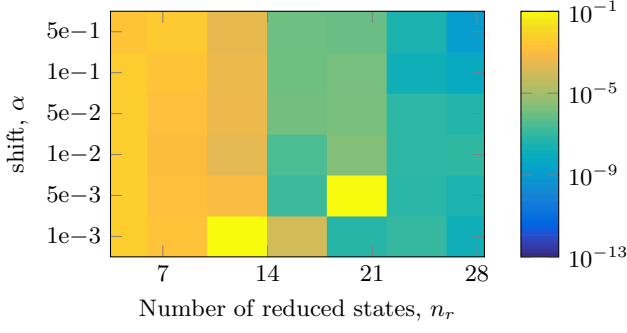
Table 1: Numbers of coupled oscillators in the EN and SM models of the IEEE 57 bus and IEEE 118 bus systems.

	EN	SM
IEEE 57 bus system	7	57
IEEE 118 bus system	54	118

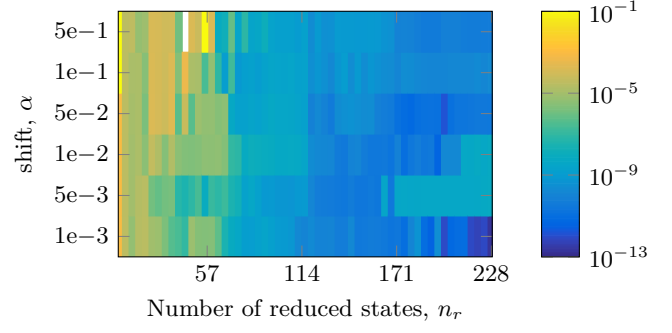
4.1 Test of the shift and number of terms

Fig. 1 shows the L^2 -norms of the output errors for reduced EN and SM models of the IEEE 57 bus system. The reduced models are obtained using the balanced truncation approach with different 1) shifts, α , of the A matrix in (20), 2) numbers of states in the reduced model, n_r , and 3) numbers of terms, N , in the approximate truncated sum (21). The simulation interval is $[0 \text{ s}, 2 \text{ s}]$.

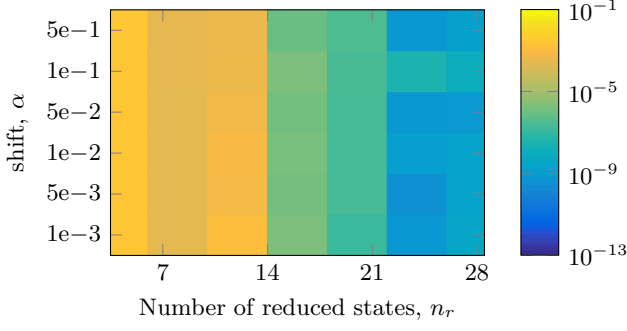
For both the EN and the SM model, N has a limited effect on the accuracy of the reduced model. For a few combinations of α and n_r , using $N = 1$ leads to very high output errors (or even simulator breakdown, indicated by a white box). For the SM model, and for very small n_r , using $N = 1$ or $N = 3$ leads to slightly lower output errors. For $N = 3$ or higher, α has almost no effect on the accuracy of the reduced EN models. For the SM model, α slightly affects the accuracy, e.g., using $\alpha \leq 0.1$ improves the accuracy for all tested N .



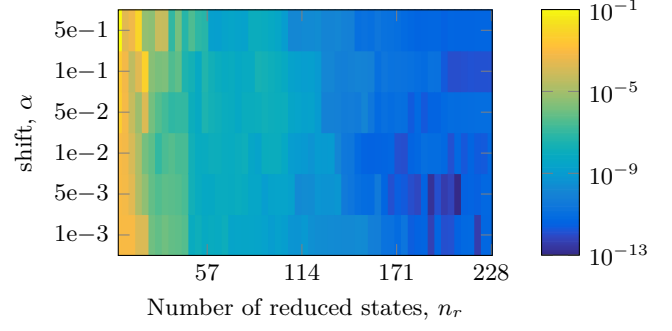
(a) The reduced EN model is obtained with $N = 1$.



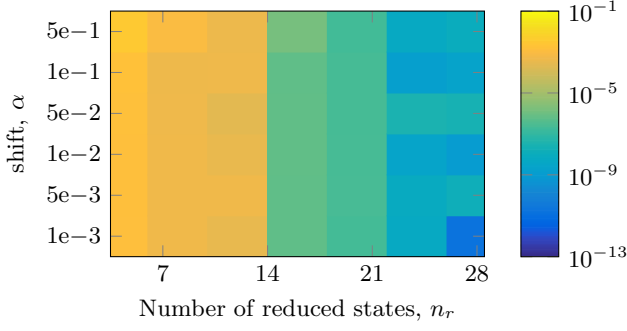
(b) The reduced SM model is obtained with $N = 1$.



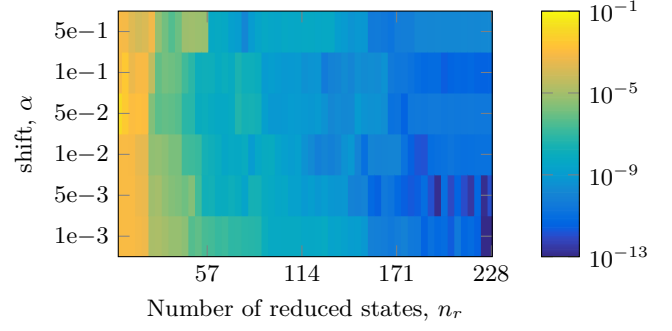
(c) The reduced EN model is obtained with $N = 3$.



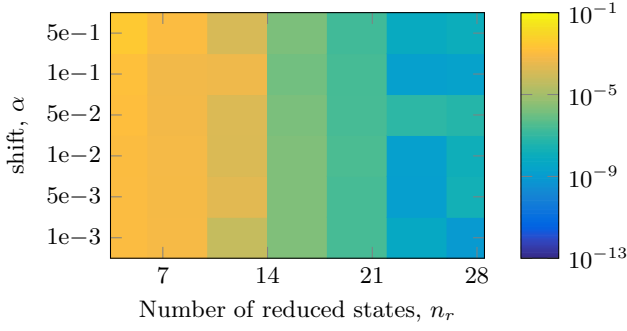
(d) The reduced SM model is obtained with $N = 3$.



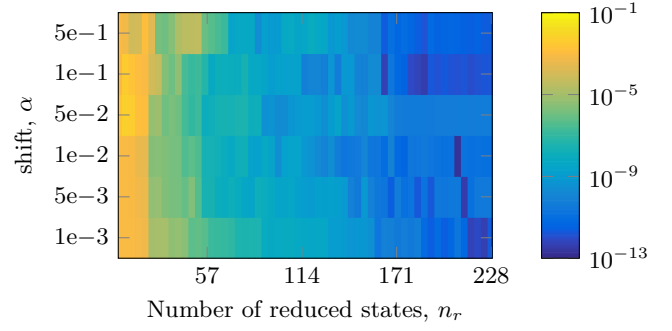
(e) The reduced EN model is obtained with $N = 5$.



(f) The reduced SM model is obtained with $N = 5$.



(g) The reduced EN model is obtained with $N = 7$.



(h) The reduced SM model is obtained with $N = 7$.

Figure 1: The L^2 -norm of the output errors for reduced EN and SM models of the IEEE 57 bus system. The reduced models are obtained using the balanced truncation approach with different 1) shifts, α , 2) numbers of reduced states, n_r , and 3) numbers of terms, N , used in approximating the Gramians.

4.2 Comparison with POD

In Fig. 2 and 3, we compare the balanced truncation approach with a basic POD approach [3, Section 9.1] for reducing the EN and SM models of the IEEE 57 bus system. We apply the POD approach to the shifted quadratic system (12). Therefore, as for the balanced truncation approach, the reduced system matrices can be computed offline using (16). We compare the L^2 -norms of 1) the output errors and 2) the Pythagorean trigonometric identity (PTI) errors (i.e., the violation of $s_i^2 + c_i^2 = 1$). As in Section 4.1, we consider different numbers of terms, N , in the approximation of the Gramians, and the simulation interval is $[0 \text{ s}, 2 \text{ s}]$. Missing points on the graphs correspond to unsuccessful simulations.

In the first test, shown in Fig. 2, we increase the initial phase angle of the first oscillator from 0 rad to 0.1 rad in the numerical simulations. In the second test, shown in Fig. 3, we increase the manipulated inputs from $u = [1; 1]$ to $u = [1.1; 1]$.

In both tests, and for both the EN and the SM model, the balanced truncation approach 1) performs equally well for all tested values of N , and 2) performs as well or better than the POD approach. Furthermore, when using the POD approach, some numerical simulations fail. This is not the case when using the balanced truncation approach.

4.3 Reduction of the IEEE 118 bus system

Fig. 4 shows the outputs and the output errors (as functions of time) for the original and the reduced EN and SM models of the IEEE 118 bus system. Based on the results in Section 4.1 and 4.2, we use a shift of $\alpha = 5 \cdot 10^{-3}$ and $N = 3$ terms in the approximation of the Gramians in the balanced truncation approach.

Both of the reduced models contain 20 state variables, corresponding to a reduction of 63% and 83% for the EN and the SM model, respectively. Despite the large reductions, the outputs for the original and the reduced models are almost indistinguishable, and the absolute output errors do not exceed 10^{-3} for the EN model and 10^{-2} for the SM model.

5 Conclusion

In this work, we describe a balanced truncation model reduction approach for reducing the nonlinear and dynamical EN and SM power grid models. In this approach, we 1) reformulate the models as quadratic systems, 2) approximate the Gramians of these systems, and 3) use block-diagonal projection matrices in the balanced truncation. We demonstrate the efficacy of this balanced truncation approach by reducing the IEEE 57 bus and IEEE 118 bus systems, and we compare it with a basic POD approach.

In future work, we will further investigate the relations between the choice of the projection matrices and 1) the ability of the reduced EN and SM models to satisfy the PTI, $\sin^2(\delta_i) + \cos^2(\delta_i) = 1$, and 2) their steady states.

Funding

We acknowledge the financial support from the German Federal Ministry of Education and Research in the project KONSENS: Konsistente Optimierung und Stabilisierung Elektrischer Netzwerksysteme (BMBF grant 05M18EVA).

A Matricization

We illustrate the concept of matricization using an example given by Kolda and Bader [18]. Let $\mathcal{H} \in \mathbb{R}^{3 \times 4 \times 2}$ be a tensor whose mode-1 matricization is

$$\mathcal{H}^{(1)} = \begin{bmatrix} 1 & 4 & 7 & 10 & 13 & 16 & 19 & 22 \\ 2 & 5 & 8 & 11 & 14 & 17 & 20 & 23 \\ 3 & 6 & 9 & 12 & 15 & 18 & 21 & 24 \end{bmatrix}. \quad (32)$$

Then, the mode-2 and mode-3 matricizations are

$$\mathcal{H}^{(2)} = \begin{bmatrix} 1 & 2 & 3 & 13 & 14 & 15 \\ 4 & 5 & 6 & 16 & 17 & 18 \\ 7 & 8 & 9 & 19 & 20 & 21 \\ 10 & 11 & 12 & 22 & 23 & 24 \end{bmatrix}, \quad (33a)$$

$$\mathcal{H}^{(3)} = \begin{bmatrix} 1 & 2 & 3 & \dots & 10 & 11 & 12 \\ 13 & 14 & 15 & \dots & 22 & 23 & 24 \end{bmatrix}. \quad (33b)$$

For more information about matricization and tensors, we refer to [18] and to previous work on model reduction of quadratic-bilinear systems [4, 5].

B Low-rank approximation

Given a matrix R for which $P = RR^T$, we denote by $\tilde{R} = \mathcal{T}_\tau(R)$ a low-rank approximation based on the singular value decomposition, $R = U\Sigma V$:

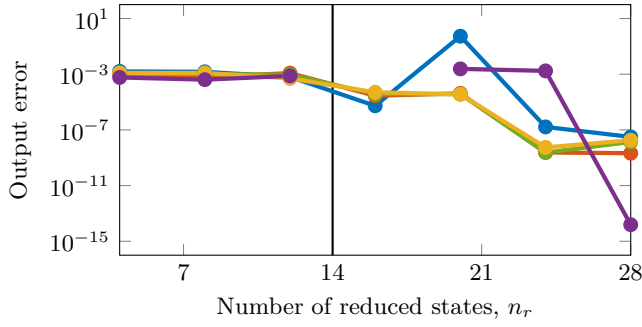
$$\tilde{R} = U\Sigma_l. \quad (34)$$

Σ_l contains the first l columns of Σ , and l is chosen such that

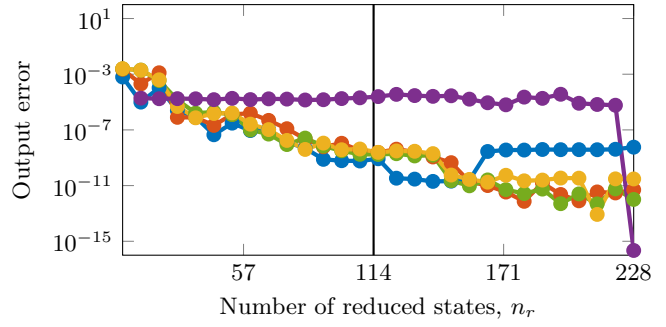
$$\sigma_i^2 > \tau\sigma_1^2, \quad (35)$$

for $i = 2, \dots, l$.

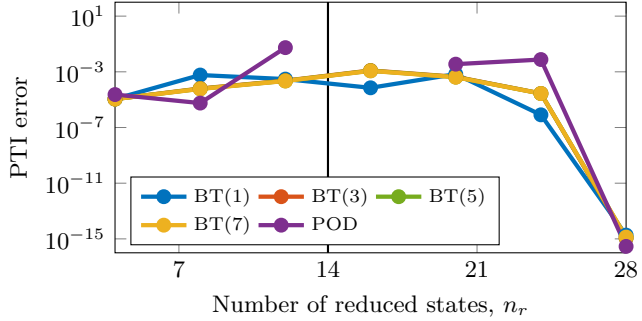
In this work, we use the machine precision as the tolerance, i.e., $\tau = 1.1102 \cdot 10^{-16}$, in order to limit the error of the low-rank approximation.



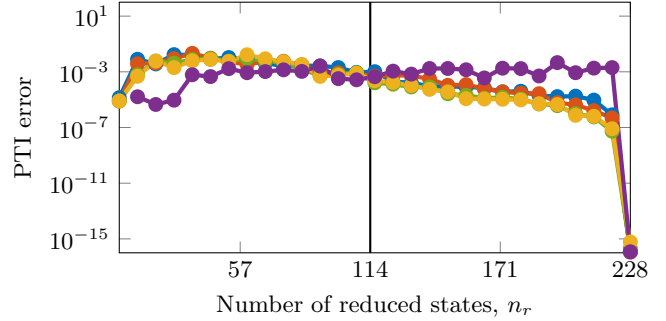
(a) Output errors for the reduced EN models.



(b) Output errors for the reduced SM models.

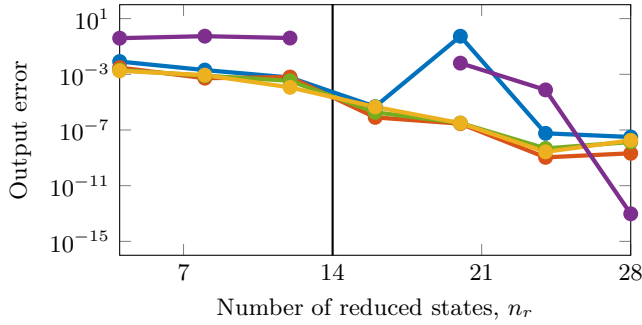


(c) PTI errors for the reduced EN models.

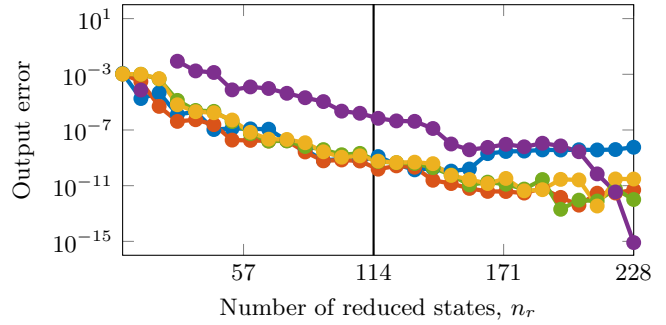


(d) PTI errors for the reduced SM models.

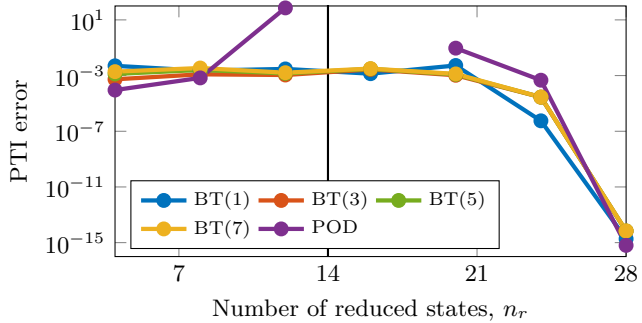
Figure 2: The L^2 -norms of the output errors for reduced EN and SM models of the IEEE 57 bus system. In the numerical simulations, we increase the initial phase angle of the first oscillator by 0.1 rad.



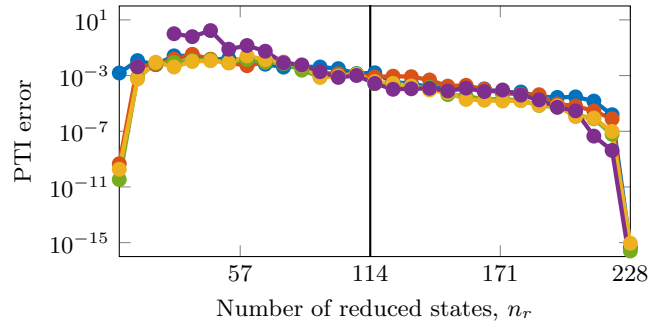
(a) Output errors for the reduced EN models.



(b) Output errors for the reduced SM models.



(c) PTI errors for the reduced EN models.



(d) PTI errors for the reduced SM models.

Figure 3: The L^2 -norms of the output errors for reduced EN and SM models of the IEEE 57 bus system. In the numerical simulations, we increase the first manipulated input by 10%, i.e., from $u = [1; 1]$ to $u = [1.1; 1]$.

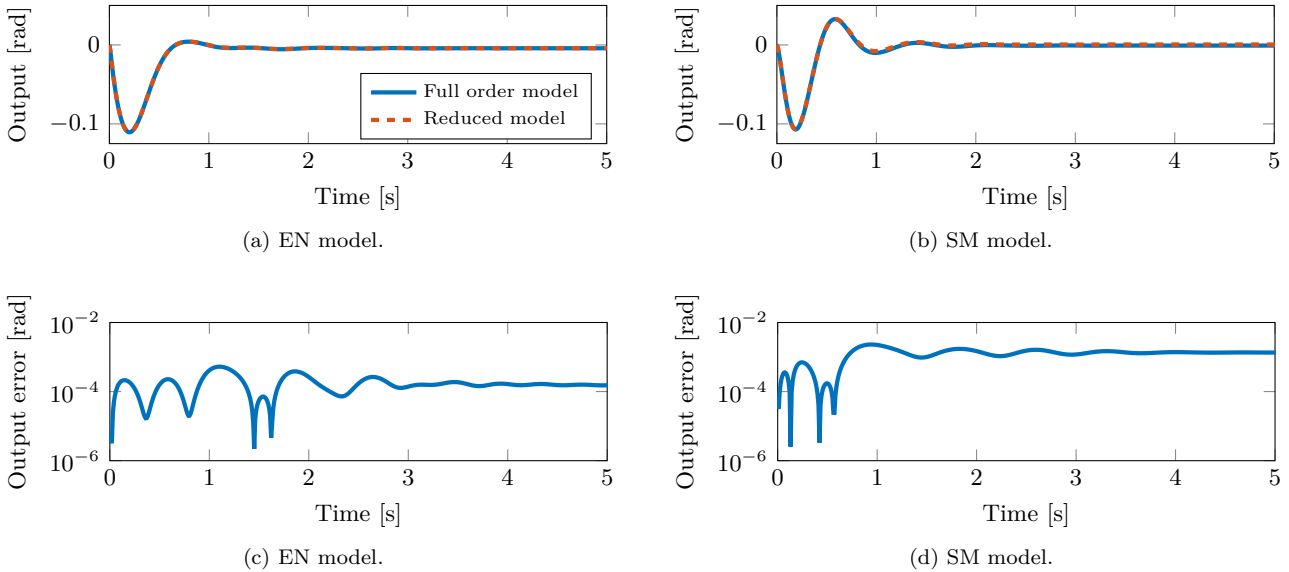


Figure 4: Top row: Outputs for the original and the reduced EN and SM models of the IEEE 118 bus system. Bottom row: The absolute difference between the output for the original the reduced order models. The reduced models contain 20 oscillators, i.e., $n_r = 80$.

C Efficient evaluation of the Kronecker products

We evaluate ΔK_{ki} in (27a) using matricization [4, 5, 18]:

$$\Delta K_{ik} = \mathcal{K}_K^{(1)}, \quad (36a)$$

$$\mathcal{K}_K^{(3)} = \tilde{R}_k \mathcal{Y}_K^{(3)}, \quad (36b)$$

$$\mathcal{Y}_K^{(2)} = \tilde{R}_{i-(k+1)} H^{(2)}. \quad (36c)$$

Similarly, we evaluate ΔL_{ki} in (27b) by

$$\Delta L_{ik} = \mathcal{K}_L^{(2)}, \quad (37a)$$

$$\mathcal{K}_L^{(3)} = \tilde{R}_k \mathcal{Y}_L^{(3)}, \quad (37b)$$

$$\mathcal{Y}_L^{(1)} = \tilde{S}_{i-(k+1)} H. \quad (37c)$$

References

- [1] Y. G. I. Acle, F. D. Freitas, N. Martins, and J. Rommes. Parameter preserving model order reduction of large sparse small-signal electromechanical stability power system models. *IEEE Transactions on Power Systems*, 34(4):2814–2824, 2019. doi: 10.1109/TPWRS.2019.2898977.
- [2] U. M. Al-Saggaf. Reduced-order models for dynamic control of a power plant with an improved transient and steady-state behavior. *Electric Power Systems Research*, 1993.
- [3] A. C. Antoulas. *Approximation of Large-Scale Dynamical Systems*, volume 6 of *Adv. Des. Control*. SIAM Publications, Philadelphia, PA, 2005. ISBN 9780898715293. doi: 10.1137/1.9780898718713.
- [4] P. Benner and T. Breiten. Two-sided projection methods for nonlinear model order reduction. *SIAM J. Sci. Comput.*, 37(2):B239–B260, 2015. doi: 10.1137/14097255X.
- [5] P. Benner and P. Goyal. Balanced truncation model order reduction for quadratic-bilinear systems. e-prints 1705.00160, arXiv, 2017. URL <https://arxiv.org/abs/1705.00160>. math.OC.
- [6] D. Chaniotis and M. A. Pai. Model reduction in power systems using Krylov subspace methods. *IEEE Transactions on Power Systems*, 20(2):888–894, 2005. doi: 10.1109/TPWRS.2005.846109.
- [7] X. Cheng and J. M. A. Scherpen. Clustering approach to model order reduction of power networks with distributed controllers. *Advances in Computational Mathematics*, 44(6):1917–1939, 2018. doi: 10.1007/s10444-018-9617-5.
- [8] A. Cherid and M. Bettayeb. Reduced-order models for the dynamics of a single-machine power system via balancing. *Electric Power Systems Research*, 22(1):7–12, 1991. doi: 10.1016/0378-7796(91)90073-V.
- [9] J. H. Chow, editor. *Power system coherency and*

- model reduction*, volume 94. Springer, 2013. doi: 10.1007/978-1-4614-1803-0.
- [10] J. H. Chow, J. R. Winkelman, M. A. Pai, and P. W. Sauer. Singular perturbation analysis of large-scale power systems. *International Journal of Electrical Power & Energy Systems*, 12(2), 1990. doi: 10.1016/0142-0615(90)90007-X.
- [11] G. H. Golub and C. F. Van Loan. *Matrix Computations*. Johns Hopkins Studies in the Mathematical Sciences. Johns Hopkins University Press, Baltimore, fourth edition, 2013. ISBN 978-1-4214-0794-4; 1-4214-0794-9; 978-1-4214-0859-0.
- [12] N. J. Higham. Computing the polar decomposition—with applications. *SIAM J. Sci. Statist. Comput.*, 7: 1160–1174, 1986.
- [13] N. J. Higham. Computing a nearest symmetric positive semidefinite matrix. *Linear Algebra Appl.*, 103: 103–118, 1988. ISSN 0024-3795. doi: 10.1016/0024-3795(88)90223-6.
- [14] J. R. Hockenberry. *Evaluation of uncertainty in dynamic reduced-order power system models*. PhD thesis, Massachusetts Institute of Technology, 2000.
- [15] R. A. Horn and C. R. Johnson. *Topics in Matrix Analysis*. Cambridge University Press, Cambridge, 1991.
- [16] S.-K. Joo, C.-C. Liu, L. E. Jones, and J.-W. Choe. Coherency and aggregation techniques incorporating rotor and voltage dynamics. *IEEE Transactions on Power Systems*, 19(2):1068–1075, 2004. doi: 10.1109/TPWRS.2004.825825.
- [17] M. Khatibi and H. Zargarzadeh. Power system dynamic model reduction by means of an iterative SVD-Krylov model reduction method. In *2016 IEEE Power & Energy Society Innovative Smart Grid Technologies Conference (ISGT)*, page 16526042, 2016. doi: 10.1109/ISGT.2016.7781027.
- [18] T. G. Kolda and B. W. Bader. Tensor decompositions and applications. *SIAM Rev.*, 51(3):455–500, 2009. ISSN 0036-1445. doi: 10.1137/07070111X.
- [19] B. Kramer and K. Willcox. Balanced truncation model reduction for lifted nonlinear systems, 2019. arXiv: 1907.12084v1.
- [20] B. Kramer and K. E. Willcox. Nonlinear model order reduction via lifting transformations and proper orthogonal decomposition. *AIAA Journal*, 57(6):2297–2307, 2019. doi: 10.2514/1.J057791.
- [21] X. Lan, H. Zhao, Y. Wang, and Z. Mi. Nonlinear power system model reduction based on empirical Gramians. In *2016 IEEE International Conference on Power System Technology (POWERCON)*, page 16487940, 2016. doi: 10.1109/POWERCON.2016.7754074.
- [22] J. Leung, M. Kinnaert, J.-C. Maun, and F. VILLELLA. Model reduction of coherent LPV models in power systems. In *2019 IEEE Power & Energy Society General Meeting (PESGM)*, page 19302246, 2019. doi: 10.1109/PESGM40551.2019.8973651.
- [23] Y. Levron and J. Belikov. Reduction of power system dynamic models using sparse representations. *IEEE Transactions on Power Systems*, 32(5):3893–3900, 2017. doi: 10.1109/TPWRS.2017.2648979.
- [24] M. H. Malik, D. Borzacchiello, F. Chinesta, and P. Diez. Reduced order modeling for transient simulation of power systems using tracetary piece-wise linear approximation. *Advanced Modeling and Simulation in Engineering Sciences*, 3:31, 2016. doi: 10.1186/s40323-016-0084-6.
- [25] X. Meng, Q. Wang, N. Zhou, S. Xiao, and Y. Chi. Multi-time scale model order reduction and stability consistency certification of inverter-interfaced DG system in AC microgrid. *Energies*, 11(1):254, 2018. doi: 10.3390/en11010254.
- [26] F. Milano and K. Srivastava. Dynamic REI equivalents for short circuit and transient stability analyses. *Electric Power Systems Research*, 79(6):878–887, 2009. doi: 10.1016/j.epsr.2008.11.007.
- [27] P. Mlinarić, T. Ishizaki, A. Chakraborty, S. Grundel, P. Benner, and J.-i. Imura. Synchronization and aggregation of nonlinear power systems with consideration of bus network structures. In *2018 European Control Conference (ECC)*, pages 2266–2271, 2018. doi: 10.23919/ECC.2018.8550528.
- [28] T. Nishikawa and A. E. Motter. Comparative analysis of existing models for power-grid synchronization. *New J. Phys.*, 17:015012, Jan. 2015. doi: 10.1088/1367-2630/17/1/015012.
- [29] D. Osipov and K. Sun. Adaptive nonlinear model reduction for fast power system simulation. *IEEE Transactions on Power Systems*, 33(6):6746–6754, 2018. doi: 10.1109/TPWRS.2018.2835766.
- [30] D. Osipov, N. Duan, A. Dimitrovski, S. Allu, S. Simunovic, and K. Sun. Adaptive model reduction for parareal in time method for transient stability simulations. In *2018 IEEE Power & Energy Society General Meeting (PESGM)*, 2018.

- [31] M. A. Pai and R. P. Adgaonkar. Singular perturbation analysis of nonlinear transients in power systems. In *1981 20th IEEE Conference on Decision and Control including the Symposium on Adaptive Processes*, pages 221–222, 1981. doi: 10.1109/CDC.1981.269515.
- [32] B. Parang, M. Mohammadi, and M. M. Arefi. Residualisation-based model order reduction in power networks with penetration of photovoltaic resources. *IET Generation, Transmission & Distribution*, 13(13): 2619–2626, 2019. doi: 10.1049/iet-gtd.2018.6172.
- [33] P. A. Parrilo, S. Lall, F. Paganini, G. C. Verghese, B. C. Lesieutre, and J. E. Marsden. Model reduction for analysis of cascading failures in power systems. In *1999 American Control Conference (ACC)*, 1999. doi: 10.1109/ACC.1999.786351.
- [34] E. Purvine, E. Cotilla-Sanchez, M. Halappanavar, Z. Huang, G. Lin, S. Lu, and S. Wang. Comparative study of clustering techniques for real-time dynamic model reduction. *Statistical Analysis and Data Mining*, 10(5):263–276, 2017. doi: 10.1002/sam.11352.
- [35] A. Ramirez, A. Mehrizi-Sani, D. Hussein, M. Matar, M. Abdel-Rahman, J. J. Chavez, A. Davoudi, and S. Kamalasan. Application of balanced realizations for model-order reduction of dynamic power system equivalents. *IEEE Transactions on Power Delivery*, 31(5):2304–2312, 2016. doi: 10.1109/TPWRD.2015.2496498.
- [36] H. Rudnick, R. I. Patino, and A. Brameller. Power-system dynamic equivalents: coherency recognition via the rate of change of kinetic energy. *IEE Proceedings C - Generation, Transmission and Distribution*, pages 325–333, 1981. doi: 10.1049/ip-c.1981.0052.
- [37] J. J. Sanchez-Gasca, J. H. Chow, and R. Galarza. Reduction of linearized power systems for the study of interarea oscillations. In *International Conference on Control Applications (CCA)*, page 5119382, 1995. doi: 10.1109/CCA.1995.555806.
- [38] G. Scarciotti. Model reduction of power systems with preservation of slow and poorly damped modes. In *2015 IEEE Power & Energy Society General Meeting*, page 15502166, 2015. doi: 10.1109/PESGM.2015.7285719.
- [39] W. H. A. Schilders, H. A. van der Vorst, and J. Rommes. *Model Order Reduction: Theory, Research Aspects and Applications*. Springer-Verlag, Berlin, Heidelberg, 2008.
- [40] K. Shomalzadeh and T. Amraee. Unstable power system model reduction using balanced truncation. In *2017 25th Iranian Conference on Electrical Engineering (ICEE)*, page 17045511, 2017. doi: 10.1109/IranianCEE.2017.7985241.
- [41] C. Sturk. *Structured model reduction and its application to power systems*. PhD thesis, KTH Royal Institute of Technology, 2012.
- [42] C. Sturk, L. Vanfretti, Y. Chompoobutrgool, and H. Sandberg. Structured power system model reduction of non-coherent areas. In *2012 IEEE Power and Energy Society General Meeting (PESGM)*, page 13170255, 2012. doi: 10.1109/PESGM.2012.6344913.
- [43] C. Sturk, L. Vanfretti, F. Milano, and H. Sandberg. Structured model reduction of power systems. In *2012 American Control Conference (ACC)*, pages 2276–2282, 2012. doi: 10.1109/ACC.2012.6315207.
- [44] C. Sturk, L. Vanfretti, Y. Chompoobutrgool, and H. Sandberg. Coherency-independent structured model reduction of power systems. *IEEE Transactions on Power Systems*, 29(5):2418–2426, 2014. doi: 10.1109/TPWRS.2014.2302871.
- [45] C. F. Van Loan. The ubiquitous Kronecker product. *Journal of Computational and Applied Mathematics*, 123:85–100, 2000. doi: 10.1016/S0377-0427(00)00393-9.
- [46] C. Wang, H. Yu, P. Li, C. Ding, C. Sun, X. Guo, F. Zhang, Y. Zhou, and Z. Yu. Krylov subspace based model reduction method for transient simulation of active distribution grid. In *2013 IEEE Power & Energy Society General Meeting*, page 13933173, 2013. doi: 10.1109/PESMG.2013.6672277.
- [47] C. Wang, H. Yu, P. Li, J. Wu, and C. Ding. Model order reduction for transient simulation of active distribution networks. *IET Generation, Transmission & Distribution*, 9(5), 2015. doi: 10.1049/iet-gtd.2014.0219.
- [48] S. Wang, S. Lu, N. Zhou, G. Lin, M. Elizondo, and M. A. Pai. Dynamic-feature extraction, attribution, and reconstruction (DEAR) method for power system model reduction. *IEEE Transactions on Power Systems*, 29(5):2049–2059, 2014. doi: 10.1109/TPWRS.2014.2301032.
- [49] S.-C. Wang, P.-H. Huang, and C.-J. Wu. Application of fuzzy C-means clustering in power system model reduction for controller design. In *5th WSEAS International Conference on Computational Intelligence, Man-machine systems and Cybernetics*, pages 223–227, 2006.

- [50] H. Weber and E. Welfonder. Dynamic model reduction for the modal analysis of frequency and power oscillations in large power systems. *IFAC Proceedings Volumes*, 21(11):233–239, 1988. doi: 10.1016/S1474-6670(17)53749-0.
- [51] F. Weiß. Simulation, analysis, and model order reduction for dynamic power network models. Master’s thesis, Otto-von-Guericke-Universität Magdeburg, 2019.
- [52] H. Zhao, X. Lan, and H. Ren. Nonlinear power system model reduction based on empirical Gramians. *Journal of Electrical Engineering*, 68(6):425–434, 2017. doi: 10.1515/jee-2017-0077.
- [53] H.-S. Zhao, N. Xue, and N. Shi. Nonlinear dynamic power system model reduction analysis using balanced empirical Gramian. *Applied Mechanics and Materials*, 448–453:2368–2374, 2013. doi: 10.4028/www.scientific.net/AMM.448-453.2368.
- [54] Z. Zhu, G. Geng, and Q. Jiang. Power system dynamic model reduction based on extended Krylov subspace method. *IEEE Transactions on Power Systems*, 31(6):4483–4494, 2016. doi: 10.1109/TPWRS.2015.2509481.
- [55] R. D. Zimmerman and C. E. Murillo-Sánchez. MATPOWER (version 6.0), 2016.
- [56] R. D. Zimmerman, C. E. Murillo-Sánchez, and R. J. Thomas. MATPOWER: Steady-state operations, planning, and analysis tools for power systems research and education. *IEEE Transactions on Power Systems*, 26(1):12–19, 2011. doi: 10.1109/TPWRS.2010.2051168.